A simplified fatigue assessment method for transverse fillet welded joints ☆

Wei Shen [a,b,*], **Renjun Yan** [a], **Nigel Barltrop** [c], **Kai Qin** [a], **Feng He** [a]

[a] Key Laboratory of High Performance Ship Technology (Wuhan University of Technology), Ministry of Education, Wuhan 430063, China
[b] State Key Laboratory of Ocean Engineering, Shanghai Jiao Tong University, Shanghai 200240, China
[c] Department of Naval Architecture and Marine Engineering, University of Strathclyde, Glasgow G40LZ, United Kingdom

ARTICLE INFO

ABSTRACT

Under the as-welded condition the fatigue crack initiation period was considered non-existent and Linear Elastic Fracture Mechanics (LEFM) was used to calculate fatigue strength for a range of weld geometries. Fracture mechanics assessment of welded joints requires accurate solutions for stress intensity factor (SIF). However, the solutions for the SIF of complex welded joints are difficult to determine due to the complicated correction factors. Three methods for SIF prediction are discussed on fillet welded specimens containing continuous or semi-elliptical surface cracks, including the traditional correction method M_k, the approximate correction method K_t, and the suggested additional crack size method ($ac+ae$). The new additional crack parameter ae is used to replace the stress concentration effect of weld profile M_k, which simplifies the calculation process. Experimental results are collected to support fatigue strength assessment of the additional crack size method.

© 2017 Published by Elsevier Ltd on behalf of Chinese Society of Theoretical and Applied Mechanics.

1. Introduction

Fatigue failure is probably the most common type of failure in welded structures. It usually initiates at the stress concentration area. Transverse fillet welded joints are often divided into two categories: non-load-carrying and load-carrying fillet welds [1]. The non-load-carrying fillet weld is defined as an attachment weld not designed to transmit the load in the main member. While for a load-carrying fillet weld, the load is transmitted through the weld and across the continuous member. In this paper, attention is focused on the non-load-carrying fillet weld, as shown in Fig. 1.

For notched specimens without any initial cracks, the fatigue life is dominated by crack initiation. However, for welded specimens containing initial cracks, the initiation life decreases greatly and the crack propagation life will dominate the fatigue life [2]. Generally, the initial defects are inevitable. Therefore, the fatigue assessment for most welded structures is focused on the crack growth portion of fatigue life and the fracture mechanics method is used to calculate the fatigue life. For non-load-carrying fillet joints, failure initiates at the
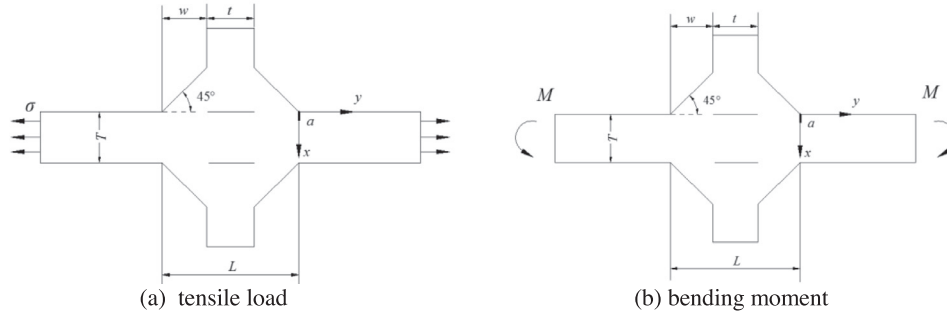
(a) tensile load

(b) bending moment

Fig. 1 – Fillet welded joint under tensile load or bending.

weld toe. In order to analyze the fatigue life, it is necessary to calculate the stress intensity factor (SIF) of the fatigue crack. Fracture mechanics assessment of these weld toe cracks requires accurate solutions for SIF. However, the solution for the SIF of a complex welded joint is difficult to obtain due to the complicated correction factors. A particular parameter of such solutions is the stress concentration factor M_k which takes into account the stress concentration due to the welded joint geometry. In this paper, the M_k factors were calculated using several different methods. Meanwhile, a new additional crack size method ($ac+ae$) for fillet welded joints was proposed to solve SIF, instead of M_k. This method treats the effect of a crack growing in a corner as an effective crack length which equals the sum of the actual crack length (ac) and an additional crack length (ae) related to the corner singularity. As an alternative to the calculation of geometric correction coefficient M_k, the additional crack can be added to the actual crack size.

2. The traditional method of fracture mechanics

2.1. Stress intensity factor K

For an infinite plate subjected to an in-plane uniform stress σ perpendicular to a central through crack of length $2a$, the fundamental equation for SIF can be presented as [3]:

$$K = \sigma \sqrt{\pi a} \tag{1}$$

Correction factors are introduced to take into account the geometry of the crack and cracked body, for a single-edge crack:

$$K = Y\sigma \sqrt{\pi a} \tag{2}$$

where Y is a function of crack length, the geometry of the cracked body and crack shape. $Y = M_k Y_u$, where M_k is a correction factor to take into account the presence of the weld; and $Y_u = M_s M_t M_p$ is the product of the free surface correction factor M_s, the finite size correction factor M_t and the crack tip plasticity correction factor M_p.

M_s depends on the crack aspect ratio, Maddox [4] suggested an approximate solution:

$$M_s = 1 + 0.12(1 - 0.75a/c) \tag{3}$$

M_t depends on the crack depth to plate thickness ratio and the crack front shape.

In the case of a fatigue crack subjected to cyclic loading ($\Delta\sigma$), the crack tip plasticity correction term was often considered as [5,6]:

$$M_p \approx \sqrt{1 + \frac{1}{13}\left(\frac{\Delta\sigma}{\sigma_Y}\right)^2} \tag{4}$$

where σ_Y is the yield limit strength.

Generally, M_p is always small for fatigue crack propagation due to nominal elastic stresses and can be ignored in most fatigue situations. Therefore, the correction factor M_p is considered in this paper.

For an elliptical crack at the toe of a fillet welded joint, SIF can be written as [4]:

$$K = \frac{M_k Y_u}{E(k)} \sigma \sqrt{\pi a} \tag{5}$$

where $E(k)$ is the second category of complete elliptic integral.

It will be seen that geometrical factor Y_u and geometric correction coefficient M_k are the two most important parameters to solve SIF. The solutions for Y_u and M_k will be discussed in turn.

2.2. Geometrical factor Y_u

Y_u is the corresponding value of Y for the same crack geometry in a plate without any welds.

As for the single-edge crack, $E(k) = 1$, Brown [7] proposed an empirical formula under tensile load:

$$Y_u = 1.122 - 0.231\alpha + 10.55\alpha^2 - 21.71\alpha^3 + 30.382\alpha^4, \ 0 < a/T \le 0.6 \tag{6}$$

where $\alpha = a/T$ is the crack length ratio.

Tada [8] also suggested an approximate formula and claimed that the resulting solution was accurate to within 0.5% for $a/T \le 0.6$:

$$Y_u = 0.265(1 - a/T)^4 + \frac{0.857 + 0.265a/T}{(1 - a/T)^{3/2}} \tag{7a}$$

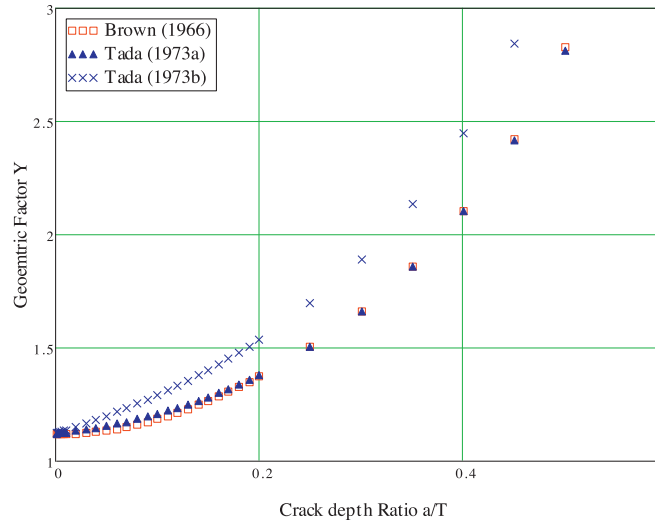And the following formula was accurate to within 1% for $a/T < 0.2$ and 0.5% for $a/T \ge 0.2$:

Fig. 2 – Y_u with different empirical formulas.

$$Y_u = \sqrt{\frac{2T}{\pi a} \tan \frac{\pi a}{2T}} \frac{0.752 + 2.02\frac{a}{T} + 0.37(1 - \sin \frac{\pi a}{2T})^3}{\cos \frac{\pi a}{2T}} \quad (7b)$$

The results of the above three experiential formulas are compared in Fig. 2.

Similarly, for a single-edge crack under bending, it was suggested by Brown [7] that function Y_u can be expressed as:

$$Y_u = 1.122 - 1.4\alpha + 7.33\alpha^2 - 13.08\alpha^3 + 14.0\alpha^4, \quad 0 < a/T \leq 0.6 \quad (8)$$

The following approximate formula was obtained by Tada [8] under bending:

$$Y_u = \sqrt{\frac{2T}{\pi a} \tan \frac{\pi a}{2T}} \frac{0.923 + 0.199(1 - \sin \frac{\pi a}{2T})^4}{\cos \frac{\pi a}{2T}} \quad (9)$$

As shown in Fig. 2, the predicted results based on Eq. (6) are similar to those based on Eq. (7a). After the comparison among these empirical formulas, Eqs. (6) and (9) are used to calculate the geometrical factor Y_u in this study for the single-edge crack under tensile load (Fig. 1a) or bending (Fig. 1b).

As for the semi-elliptical surface crack, Newman and Raju [9,10] presented an empirical equation for SIF as follows:

$$K_I = (\sigma_t + H\sigma_b)F\left(\frac{a}{T}, \frac{a}{c}, \frac{c}{w}, \phi\right)\frac{\sqrt{\pi a}}{E(k)} \quad (10)$$

where H is a function of crack depth ratio a/T, aspect ratio a/c, and parametric angle φ; geometric factor Y_u is expressed in function F; σ_t is the tensile stress and σ_b is the bending stress at the surface.

2.3. Geometric correction coefficient M_k

M_k is the stress concentration magnification factor which is defined as the ratio of the stress intensity factor of a cracked plate with stress concentration to the SIF of the same cracked plate without stress concentration.

For different joint forms, the empirical formulas of M_k are often different and complicated.

For the butt-welded plate with a thickness of T, the modifying factor can be calculated approximately as follows [11]:

$$\begin{cases} M_k = (5\frac{a}{T})^{-q} & (0 \leq a \leq 0.2t) \\ M_k = 1 & (a \geq 0.2t) \end{cases} \quad (11)$$

where $q = \lg(11.584 - 0.0588\theta)/2.30$, and θ is the weld toe angle.

Fu and Haswell [12] suggested the expression of M_k for the surface crack of T joint:

$$M_{k,t} = 0.9755 + 1.7261\left(1.0 + 76.9069\frac{a}{T}\right)^{-1.2879} \quad (12a)$$

$$M_{k,b} = 0.9249 + 2.9041\left(1.0 + 266.4478\frac{a}{T}\right)^{-0.7916} \quad (12b)$$

where t refers to tension, and b refers to bending.

Considering the geometric parameters of T joint, Bowness and Lee [13,14] provided the approximate formula based on the Finite Element (FE) method:

$$M_k = f_1\left(\frac{a}{T}, \frac{a}{c}\right) + f_2\left(\frac{a}{T}, \theta\right) + f_3\left(\frac{a}{T}, \theta, \frac{L}{T}\right) \quad (13)$$

where f_1, f_2 and f_3 are very complex polynomials. Although Han [15] simplified the above formula according to the main influence factors, the expression is still tedious.

As for fillet welded joints, Hayes [16] provided SIF solutions for edge cracks (Fig. 1). He calculated the non-dimensional SIF $K/[\sigma\sqrt{(\pi a)}]$, i.e. Y_uM_k, for different crack lengths. The solutions of Y_u were analyzed using an edge-cracked plate without stress concentration, then it was easy to separate the values of M_k.

In order to simplify the analytical process, Maddox [4] proposed an approximate evaluation method based on the superposition principle. As shown in Fig. 3, the superposition method assumes that the stress distribution along the cracked plane is equivalent to that in an edge-cracked plate without a fillet (Fig. 3a), $M_k = 1$, plus that across a crack-free plate of the original geometry (Fig. 3b). In other words, the SIF for the crack of fillet joint (Fig. 1) is magnified by the same amount as that

(a) An edge-cracked plate without a fillet
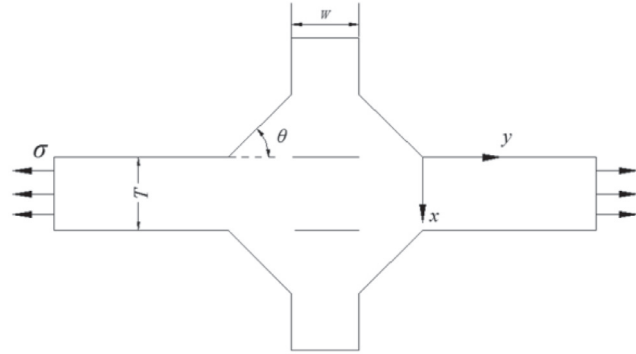
(b) A crack-free plate of the original geometry

Fig. 3 – Superposition principle of fillet joints.

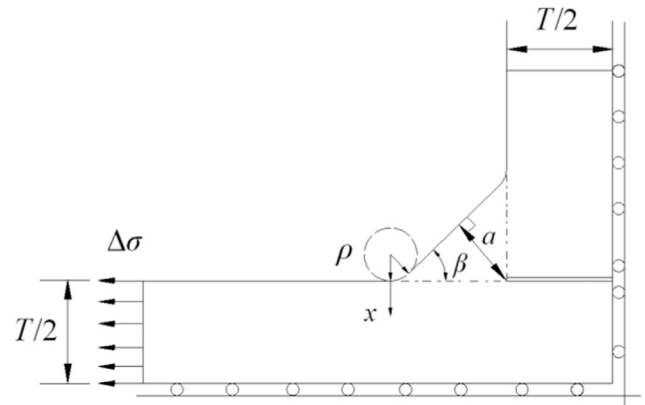| Table 1 – Comparison between M_k and K_t for a 45° fillet.			
a/T	K_t	M_k	$(M_k - K_t)/M_k \times 100\%$
0	2.80	2.80	0
0.05	1.27	1.27	0
0.075	1.13	1.20	5.8
0.10	1.05	1.16	9.5
0.15	0.95	1.12	15.1
0.20	0.91	1.08	15.75
0.25	0.88	1.04	15.4
0.30	0.87	1.01	13.8
0.40	0.84	1.00	16
0.50	0.84	1.00	16

Fig. 4 – A more complex fillet joint.

for the uncracked plate (Fig. 3b) at a position corresponding to the crack length, $M_k = K_t$ at $x = a$. However, the error is obvious since the presence of a crack would modify the stress distribution due to the stress concentration at crack tip.

The method above would provide useful means to obtain the approximate solutions of M_k if the error is small. Generally, for very small cracks, $M_k \approx K_t$. The value of M_k is therefore set equal to K_t when $a/T = 0$. With the increase of crack, the stress field of crack tip will become stable and the value of M_k will reduce to 1. However, the notch stress concentration factor K_t is relative to the uncracked body and $K_t = \sigma_t/\sigma_0$ may decrease further. The values of K_t and M_k for a 45° fillet are compared in Table 1.

It can be seen in Table 1 that the error could be up to 16%. This confirms that SIF can be overestimated if it is assumed that $M_k = K_t$. However, for some approximate analyses, this accuracy may be sufficient.

For more complex fillet joints, as shown in Fig. 4, the weld flank angle β and weld toe radius ρ were introduced to calculate M_k. The fitted M_k was presented by Eq. (14) [17]:

$$M_k = \frac{1 + s_1\left(\frac{2x}{T}\right)}{s_2 + s_3\left(\frac{2x}{T}\right)^{s_4}} \tag{14}$$

where $s_i = \dfrac{r_{1,i} + r_{2,i}\left(\frac{\rho}{T}\right)^{r_{3,i}}}{r_{4,i} + \left(\frac{\rho}{T}\right)^{r_{3,i}}}$, $r_{i,j} = \dfrac{a_{i,j} + b_{i,j}\left(\frac{\pi}{180}\beta\right)^{c_{i,j}}}{d_{i,j} + \left(\frac{\pi}{180}\beta\right)^{c_{i,j}}}$, and the parameters $a_{i,j}$, $b_{i,j}$, $c_{i,j}$, and $d_{i,j}$ are presented in literature [17].

The SIF and the magnification factor M_k are analyzed above. Obviously, the empirical formulas of M_k are often difficult and complicated to calculate due to the changes in joint forms. Based on notch stress strength theory, a simplified model is proposed in this paper to solve the SIF of transverse fillet welded joints.
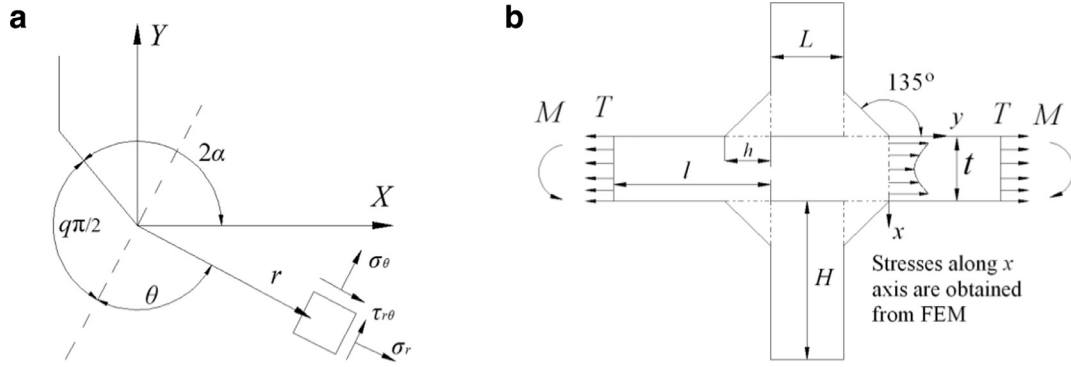
Fig. 5 – Joint geometry of 135° welded joint.

3. The method of additional crack size

3.1. Notch stress strength theory

Williams [18] stated that the stress field is singular at the crack tip. In a polar frame of reference (r, θ), the stress field at the corner is the summation of Mode I and Mode II stresses.

$$\begin{Bmatrix} \sigma_\theta \\ \sigma_r \\ \tau_{r\theta} \end{Bmatrix} = \lambda_1 r^{\lambda_1 - 1} a_1 \begin{Bmatrix} f_{1,\theta}(\theta) \\ f_{1,r}(\theta) \\ f_{1,r\theta}(\theta) \end{Bmatrix} + \lambda_2 r^{\lambda_2 - 1} a_2 \begin{Bmatrix} f_{2,\theta}(\theta) \\ f_{2,r}(\theta) \\ f_{2,r\theta}(\theta) \end{Bmatrix} \tag{15}$$

where r is the distance to the corner, $f_i(\theta)$ are described in Eq. (17) and the eigenvalues λ_i are determined by Eq. (16).

$$\sin(\lambda_i q\pi) + \lambda_i \sin(q\pi) = 0 \tag{16}$$

Parameters around the 135° corner can be defined, as shown in Fig. 5.

The stress component for Mode I, tension, is:

$$\begin{Bmatrix} \sigma_\theta \\ \sigma_r \\ \tau_{r\theta} \end{Bmatrix} = \frac{1}{\sqrt{2\pi}} \frac{r^{\lambda_1 - 1} K_1}{[(1+\lambda_1) + \chi_1(1-\lambda_1)]} \left[\begin{Bmatrix} (1+\lambda_1)\cos(1-\lambda_1)\theta \\ (3-\lambda_1)\cos(1-\lambda_1)\theta \\ (1-\lambda_1)\sin(1-\lambda_1)\theta \end{Bmatrix} \right.$$
$$\left. + \chi_1(1-\lambda_1) \begin{Bmatrix} \cos(1+\lambda_1)\theta \\ -\cos(1+\lambda_1)\theta \\ \sin(1+\lambda_1)\theta \end{Bmatrix} \right] \tag{17}$$

for Mode II, shear, is:

$$\begin{Bmatrix} \sigma_\theta \\ \sigma_r \\ \tau_{r\theta} \end{Bmatrix} = \frac{1}{\sqrt{2\pi}} \frac{r^{\lambda_2 - 1} K_2}{[(1-\lambda_2) + \chi_2(1+\lambda_2)]} \left[\begin{Bmatrix} (1+\lambda_2)\sin(1-\lambda_2)\theta \\ (3-\lambda_2)\sin(1-\lambda_2)\theta \\ (1-\lambda_2)\cos(1-\lambda_2)\theta \end{Bmatrix} \right.$$
$$\left. + \chi_2(1+\lambda_2) \begin{Bmatrix} \sin(1+\lambda_2)\theta \\ -\sin(1+\lambda_2)\theta \\ \cos(1+\lambda_2)\theta \end{Bmatrix} \right] \tag{18}$$

where $K_i = \sigma_0 \cdot k_i \cdot t^{1-\lambda_i}$; k_i is a function of h, t, L; σ_0 is the nominal tensile or shear stress; and K_i is the N-SIF value defined by Lazzarin and Tovo [19–21].

3.2. Modified singularity strength method

The axial stress distribution of Mode I at a corner can be simplified as:

$$\sigma_{\theta 1} = \frac{\sigma_0}{\sqrt{2\pi}} \frac{1}{x^{p_1}} [C_1(\alpha, \theta) f_1(h, t, L)^{1/p_1} t]^{p_1} \tag{19a}$$

And for Mode II:

$$\sigma_{\theta 2} = \frac{\sigma_0}{\sqrt{2\pi}} \frac{1}{x^{p_2}} \left[C_2(\alpha, \theta) f_2(h, t, L)^{1/p_2} t \right]^{p_2} \tag{19b}$$

where x is the distance to the corner;

$$C_1(\alpha, \theta) = \left[\frac{(1+\lambda_1)\cos(1-\lambda_1)\theta + \chi_1(1-\lambda_1)\cos(1+\lambda_1)\theta}{(1+\lambda_1) + \chi_1(1-\lambda_1)} \right]^{\frac{1}{p_1}};$$

$$C_2(\alpha, \theta) = \left[\frac{(1+\lambda_2)\sin(1-\lambda_2)\theta + \chi_2(1+\lambda_2)\sin(1+\lambda_2)\theta}{(1-\lambda_2) + \chi_2(1+\lambda_2)} \right]^{\frac{1}{p_2}};$$

$f_i(h, t, L) = k_i$; and $p_i = 1 - \lambda_i$. For different corner angels, the parameters can be extracted from literature [11].

For a given corner (2α), p_i and $C_i(\alpha, \theta)$ are constants; and k_i is a function of h, t, L. Taking all the constants into k_i, a new function can be defined as $as_i = C_i(\alpha, \theta) f_i(h, t, L)^{\frac{1}{p_i}} t\pi^{\frac{1}{2p_i}}$, then Eq. (19) becomes Eq. (20):

$$\sigma_{\theta 1} = \frac{\sigma_0}{\sqrt{2}} \left(\frac{as_1}{x} \right)^{p_1} \tag{20a}$$

$$\sigma_{\theta 2} = \frac{\sigma_0}{\sqrt{2}} \left(\frac{as_2}{x} \right)^{p_2} \tag{20b}$$

$$\sigma_\theta = \sigma_{\theta 1} + \sigma_{\theta 2} = \frac{\sigma_0}{\sqrt{2}} \left[\left(\frac{as_1}{x} \right)^{p_1} + \left(\frac{as_2}{x} \right)^{p_2} \right] \tag{21}$$

where 'as' is introduced and named as singularity strength to describe the singular stress field at the corner.

For a given corner, it can be seen that as long as the strength singularity values 'as_i' are known, the stress distribution along thickness at the corner will be determined by Eq. (21). Within the investigation range of $0 < L/t \leq 3.0$ and $0 < 2h/t \leq 1$, the FE models were employed to analyze the influence of the attachment geometry. The dimensions (L, H) of the attachment were changed from 0.5 m to 3 m; the length of the main plate l was fixed at 2 m (meeting the requirement of providing uniform stress field near the corner), and the width t was changed from 1 m to 4 m [22,23]. Values of the 'as_i' were fitted using the
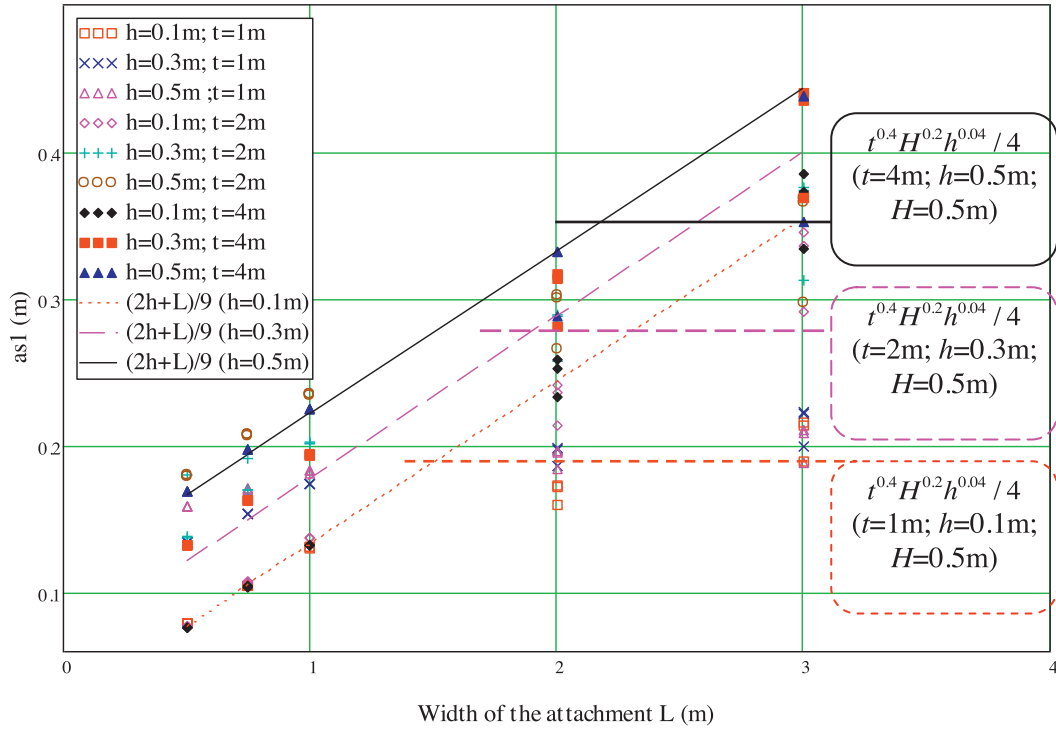
Fig. 6 – The prediction of 'as_1' under tensile loading.

method of least-squares with a polynomial function based on the numerical data. The results show that the 'as_1' value can be determined by two approximate formulas, and the smaller of the two approximate formulas is closer to the numerical results, as shown in Figs. 6–7.

Expressions of as_1 and as_2 for transverse non-load-carrying fillet weld are fitted as follows: Tensile:

$$as_1 = \min\left(\frac{t^{0.4}H^{0.2}h^{0.04}}{4}, \frac{2h+L}{9}\right) \quad (22a)$$

$$as_2 = \frac{2h+L}{0.33} \quad (22b)$$

Bending:

$$as_1 = \min\left(\frac{2t+L}{40}, \frac{4h+L}{12}\right) \quad (23a)$$

$$as_2 = \frac{2h+L}{0.36} \quad (23b)$$

where t is the width of main plate, L is the width of attachment, H is the length of attachment and h is the height of bracket (see Fig. 5).

3.3. Concept of additional crack size

Validity of the above method was further verified in literature [22]. As soon as as_1 and as_2 are known, the relevant stress distribution can be easily computed by Eq. (21).When Mode I stress is dominant, Mode II stress is often ignored. At 0° (an edge crack), $p_1 = 0.5$ and the stress decreases at x from the corner, in proportion to $1/x^{0.5}$. At 90°, p_1 reduces to 0.455. And at

135°, p_1 is 0.326. Stress plots for different corner angles are shown in Fig. 8(a).

As shown in Fig. 8(b), the notch stress field distribution and trend are very similar for 0° and 90° corners. Therefore, the additional crack size method treats the effect of a crack growing in a 90° corner as an effective crack length which equals the sum of the actual crack length (ac) and an additional crack length (ae) related to the corner singularity, as demonstrated in Fig. 9.

This additional crack length (ae) can be defined for any actual crack length and ($ac+ae$) is calculated to give the same stress intensity factor as that of the corner crack. The method of additional crack size can be represented as follows:

$$K = Y_u\sigma\sqrt{\pi(ac+ae)} \quad (ac > 0) \quad (24)$$

The additional crack length depends on the nature of the corner singularity p as well as the size of the crack relative to the singularity strength value (as) given in Eq. (20). By definition, the singularity strength 'as' is introduced to describe the singular stress field at the corner. Therefore, the additional crack length can be approximately estimated from the value of as by $ae \approx as$ [24].

Based on the above assumption, a similar formula for fillet joints could be expressed as:

$$K = Y_u\sigma\sqrt{\pi(ac+nas)} \quad (ac > 0) \quad (25)$$

where as is calculated by the simple formulas in Eqs. (22) and (23), and the coefficient n is defined as the attenuation coefficient due to a smaller singularity exponent p_1. For the 135°
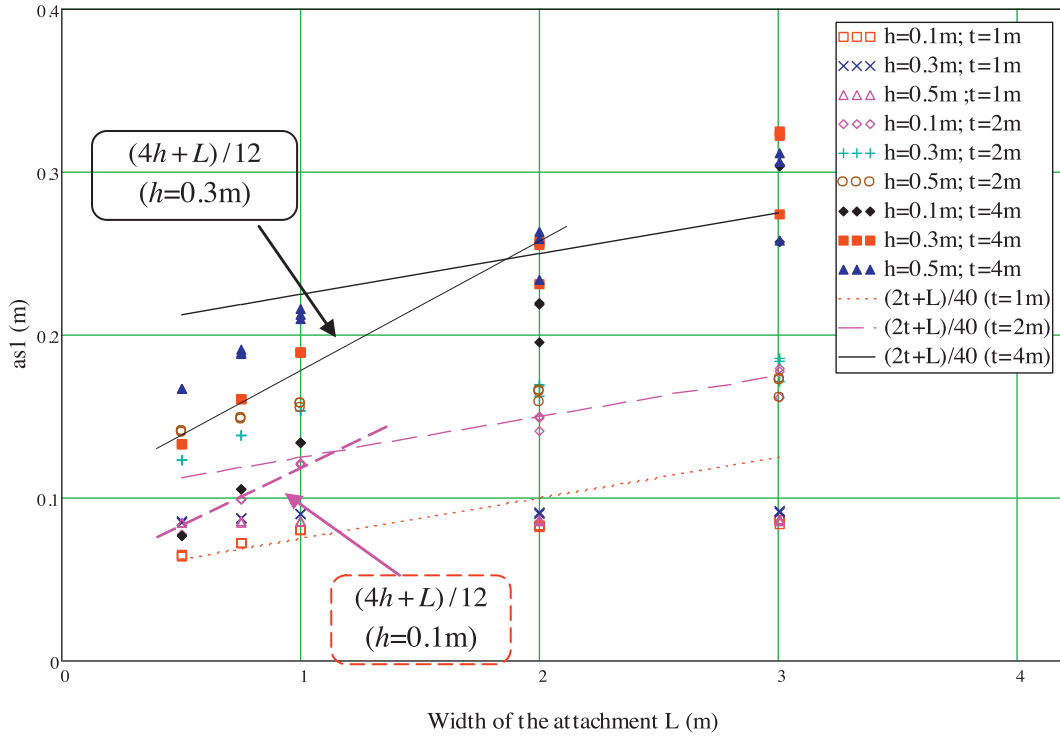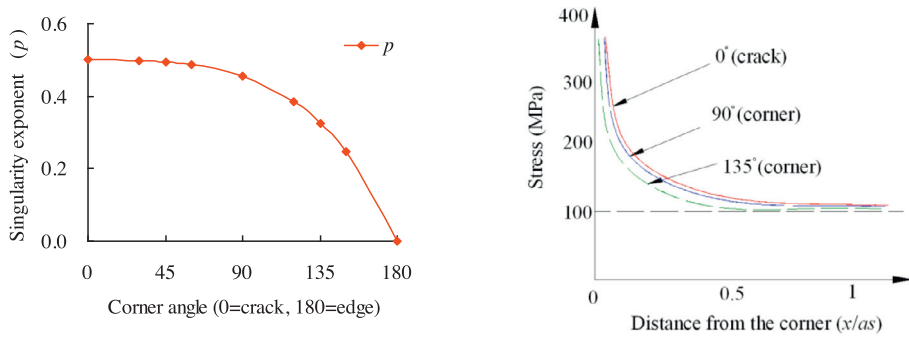
Fig. 7 – The prediction of 'as_1' under bending.

(a) Variation of p with corner angle   (b) Stress field comparison (nominal stress σ_0 =100 MPa)

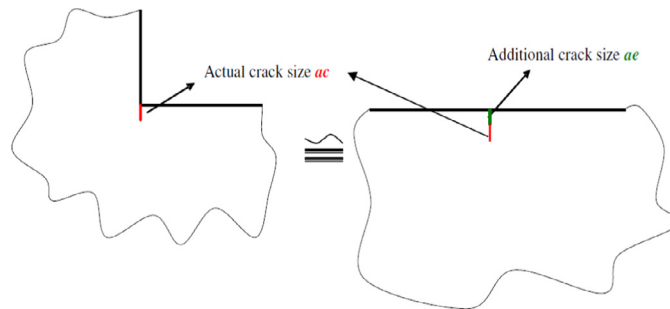Fig. 8 – The stress field distribution for different corner angles.

Fig. 9 – Concept of additional crack size.

corner, $n = 0.25$ is suggested by analyzing a series of models using the FE method [25].

The new additional crack parameter is used to replace the stress concentration effect of weld profile, which simplifies the calculation process.

4. Crack propagation life analysis

As one of the most important fatigue crack growth models, the Paris formula is commonly used in practice, which is also recommended by IIW and BS 7608 for calculating the fatigue crack propagation rate of welded joints made of steel or aluminum.

$$\frac{\mathrm{d}a}{\mathrm{d}N} = C\Delta K^m \tag{26}$$

where $\mathrm{d}a/\mathrm{d}N$, in mm/cycle, is the crack growth rate; ΔK is the range of SIF; and C and m are material constants. The constants $C_{mean} = 1.7 \times 10^{-13}$, $C_{char} = 5.21 \times 10^{-13}$ and $m = 3.0$ are recommended by IIW [26]. C_{mean} is the mean fatigue crack growth rate coefficient and C_{char} is the value considering 95% survival probability.

The mean value of C is suggested in BS 7608 by the equation [27]:

$$C_{mean} = \frac{1.315 \times 10^{-4}}{895^m}, \quad R = 0 \tag{27}$$

When $m = 3.0$, $C_{mean} = 1.1834 \times 10^{-13}$. It is also recommended that the calculated value of C should be multiplied by 2 to consider the scatter, i.e. $C_{char} = 2.367 \times 10^{-13}$, $m = 3.0$.

If the crack length is normalized by the plate thickness, a/T, the fatigue life is obtained by integrating Eqs. (2) and (26).

$$N = \int_{\frac{a_i}{T}}^{\frac{a_f}{T}} \frac{1}{C} \Delta K^{-m} T \mathrm{d}\left(\frac{a}{T}\right) = \int_{\frac{a_i}{T}}^{\frac{a_f}{T}} \frac{1}{C}\left(M_k Y_u \Delta\sigma \sqrt{\pi T \cdot \frac{a}{T}}\right)^{-m} T \mathrm{d}\left(\frac{a}{T}\right) \tag{28}$$

Separating the parameters, one has:

$$\int_{\alpha_i}^{\alpha_f} (M_k Y_u \sqrt{\pi\alpha})^{-m} \mathrm{d}\alpha = C(\Delta\sigma)^m T^{m/2-1} N \tag{29}$$

where $\alpha = a/T$, $\alpha_i = a_i/T$, $\alpha_f = a_f/T$, a_i is the initial crack depth and α_f is the final crack depth. Eq. (29) can also be written as:

$$\left\{\Delta\sigma\left(\frac{T^{m/2-1}}{I}\right)^{1/m}\right\}^m N = \frac{1}{C} \tag{30}$$

where I is $\int_{\alpha_i}^{\alpha_f} (M_k Y_u \sqrt{\pi\alpha})^{-m} \mathrm{d}\alpha$; and the expression $\Delta\sigma\left(\frac{T^{m/2-1}}{I}\right)^{1/m} = \Delta\sigma^*$ is defined as the equivalent structural stress range or the generalized stress parameter by Gurney [28] and Dong [29]. This equivalent parameter reflects the effect of stress gradient due to specimen geometry.

5. Analysis of estimated results

For the purpose of fatigue design, welded joints are often divided into a series of Classes, with different designed S-N curves. The basic S-N curves are defined as follows [27]:

$$\log(N) = \log(k_1) - d\sigma - m\log(S_B) \tag{31}$$

where k_1 is a constant; σ is the standard deviation of $\log(N)$; d is the number of standard deviations below the mean S-N curve, $d = 2$ for 97.7% survival probability; and m is the inverse slope of S-N curve.

To validate the above proposed method, fatigue test results [30] are collected for several non-load-carrying fillet welded joints shown in Fig. 1. Fatigue tests were performed on 16 series under tensile load and 7 series under bending for both continuous cracks and semi-elliptical cracks, as shown in Table 2.

It is well known that the fracture mechanics based computations are extremely sensitive to the initial crack size. In all cases it was assumed that the initial defect at the weld toe a_i was 0.15 mm, this being typical of the average values which have been recommended in literature [30]. The final crack size α_f was assumed to be $T/2$. The initial semi-elliptical cracks were assumed to be semi-circular with the length $2c_0 = 0.3$ mm and the depth $a_0 = 0.15$ mm. The experimental crack aspect ratio curve proposed by Engesvik and Moan [31] was used for the growing semi-elliptical surface cracks:

$$\frac{a}{2c} = \begin{cases} 0.5 & (a < 0.062 \text{ mm}) \\ 1/(6.43 - 0.27/a) & (0.062 \leq a \leq 3 \text{ mm}) \\ 0 & (a > 3 \text{ mm}) \end{cases} \tag{32}$$

In the analyses, the value of Y_u for continuous crack was taken to be Eqs. (6) and (9) defined by Brown [7] and Tada [8]. As for the semi-elliptical crack, Y_u was calculated by Eq. (10) proposed by Newman and Raju [9,10].

Three methods for SIF prediction were discussed on the above fillet welded specimens: the traditional geometric coefficient correction method M_k, the approximate stress concentration factor method K_t and the new additional crack size method $(ac+ae)$.

The correction coefficients M_k were those defined by Smith and Gurney [30]. The notch stress field formulas of 135° sharp corners proposed by Shen and Barltrop [22] were used to calculate the values of $K_t = \sigma_t/\sigma_0$. The corresponding additional crack lengths (ae) were given in Eqs. (22)-(23).

The corresponding values of C and m in Eq. (28) refer to standards BS 7608 and IIW:

$$\begin{cases} m = 3.0, & C = 2.367 \times 10^{-13} \text{(BS 7608)} \\ m = 3.0, & C = 5.21 \times 10^{-13} \text{(IIW)} \\ \text{Actual } m, & C = 1.315 \times 10^{-4}/895^m \end{cases} \tag{33}$$

where the actual m is fitted by experimental data in literature [30], as shown in Table 2.

The predicted and experimental results of fatigue strength at 2×10^6 cycles with three methods are summarized in Fig. 10. The fatigue strengths derived from the approximate stress concentration factor method K_t, the new additional

Table 2 – Summary of fatigue strength for cruciform welded specimens ($R \approx 0$, $N = 2 \times 10^6$ cycles).

Series	Specimens [30]	Load type	Width of main plate t (mm)	Width of attachment L (mm)	Height of bracket h (mm)	The inverse slope m	Fatigue strengths at 2×10^6 cycles (MPa)
1	Cruciform	T	13	3	5	3.367	122.4
2	Cruciform	T	13	10	8	3.358	100.9
3	Cruciform	T	25	3	5	3.340	124.6
4	Cruciform	T	25	32	9	3.179	88.5
5	Cruciform	T	38	13	8	3.103	93.1
6	Cruciform	T	38	220	15	2.430	67.7
7	Cruciform	T	100	3	5	3.697	124.7
8	Cruciform	T	100	220	15	2.914	54.9
9	Cruciform	T	13	13	8	3.469	97.4
10	Cruciform	T	13	13	10	3.744	95.8
11	Cruciform	T	25	25	16	2.711	85.6
12	Cruciform	T	38	38	10	3.139	80.9
13	Cruciform	T	38	50	10	3.299	81.7
14	Cruciform	T	13	10	8	3.701	102.3
15	Cruciform	T	50	50	16	3.563	79.4
16	Cruciform	T	100	50	16	3.234	73.7
17	Cruciform	B	6.4	13	8	4.050	154.8
18	Cruciform	B	8	13	8	3.374	130.6
19	Cruciform	B	13	13	10	3.599	127.6
20	Cruciform	B	13	13	5	3.200	125.8
21	Cruciform	B	13	38	10	3.246	119.1
22	Cruciform	B	25	38	10	3.100	102.2
23	Cruciform	B	38	13	10	3.427	112.5

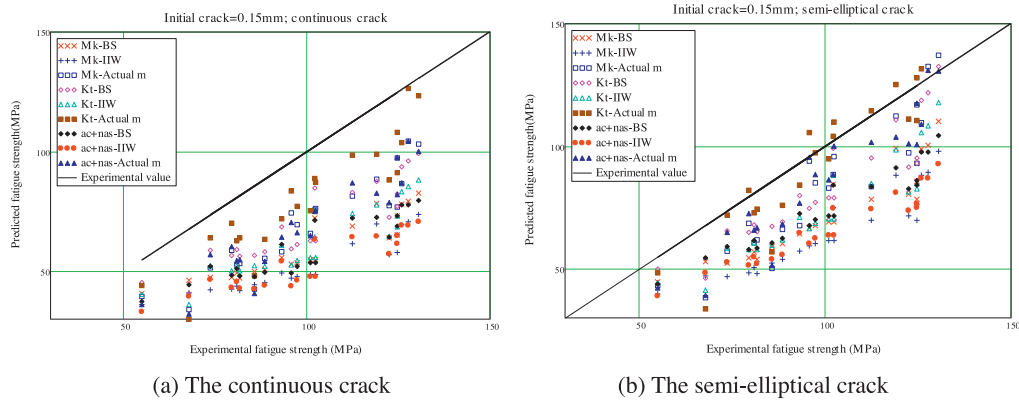(a) The continuous crack   (b) The semi-elliptical crack

Fig. 10 – Predicted and experimental results of fatigue strengths with three methods.

crack size method (ac+ae) and those calculated by the traditional geometric coefficient correction method M_k are shown in Fig. 11. The following observations are drawn based on the comparative analysis of Figs. 10–11.

(1) The values of C and m from BS 7608 and IIW are different. The results from IIW tend to be more conservative. However, all the predicted results have considered the 95% survival probability. Most of the data are below FAT 90, the reference fatigue strength recommended by IIW [26].

(2) Comparative calculations show that the predicted fatigue strengths are very sensitive to the crack forms. The strength of a joint with a semi-circular crack is approximately 30% greater than that of the same joint with a continuous crack.

(3) As shown in Fig. 11, the strength errors with methods M_k and (ac+ae) are very close. The maximum relative error with the (ac+ae) method does not exceed 10%, and most of the errors are within 5%.

(4) It is concluded that the maximum relative error introduced by assuming $M_k \approx K_t$ could be up to 20%. However, this accuracy may be acceptable for some approximate analyses, and the calculation process will be simplified effectively.

6.   Conclusions

The geometrical factor Y_u and geometric correction coefficient M_k are the most important parameters to solve SIF of the complex welded joints. On the basis of theoretical calculations and
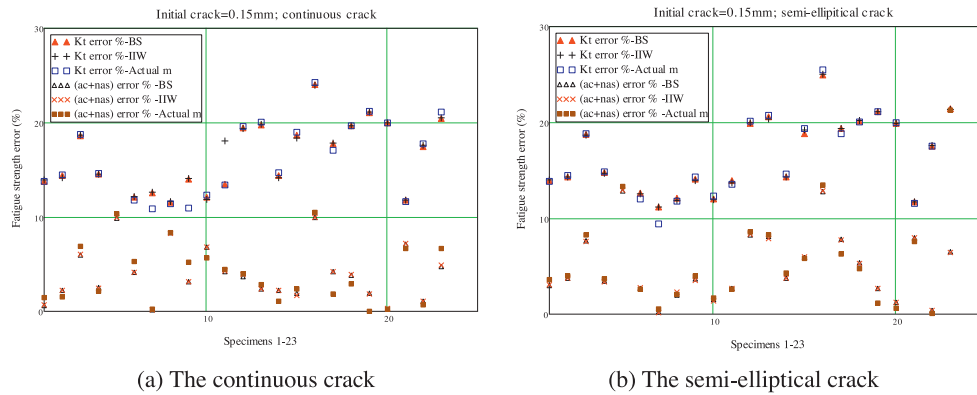
(a) The continuous crack (b) The semi-elliptical crack

Fig. 11 – The relative errors compared with the results of the traditional correction method M_k.

comparisons between predictions and experimental results, the following conclusions can be made:

(1) It has been confirmed that the fatigue strength of transverse non-load-carrying fillet joints are very sensitive to both the assumed values of C and m and the assumed crack forms. The strength of the joint with a semi-circular crack is approximately 30% greater than that of the same joint with a continuous crack. It is concluded that the continuous crack is more dangerous than the semi-circular crack.

(2) When $a/T = 0$, $M_k = K_t$. With the increase of crack depth, the stress field of crack tip will become stable and the value of M_k will reduce to 1. However, the notch stress concentration factor K_t is relative to the uncracked body and $K_t = \sigma_t/\sigma_0$ may decrease further. Therefore, the predicted fatigue strengths of K_t are greater than those of the same joints with the correction of M_k. Experimental results show that the maximum relative error introduced by assuming $M_k \approx K_t$ could be up to 20%, compared with the results of the traditional correction method M_k.

(3) The fatigue strengths derived from the traditional coefficient correction method M_k and the new additional crack size method $(ac+ae)$ are compared. The maximum relative error does not exceed 10%. The results show that the new additional crack size method based on the notch stress strength theory has the advantage in simple and accurate fatigue strength estimation for transverse fillet welded joints.

Acknowledgments

REFERENCES

[1] S.T. Lie, Analysis of fatigue strength on non-load-carrying and load-carrying fillet welded joints, J. Strain Anal. 29 (4) (1994) 243–255.
[2] T. Nykänen, G. Marquis, T. Björk, A simplified fatigue assessment method for high quality welded cruciform joints, Int. J. Fatigue 31 (2009) 79–87.
[3] G.R. Irwin, The crack extension force for a part through crack in a plate, J. Appl. Mech. 29 (1962) 651–654 ASME.
[4] S.J. Maddox, An analysis of fatigue cracks in fillet welded joints, Int. J. Fract. 11 (2) (1975) 221–243.
[5] J.R. Rice, Plastic yielding at a crack tip, in: Proceedings of 1st Conference on Fracture, Sendai, 1965.
[6] J. Schijve, Cumulative damage problems in aircraft structures and materials, Aeronaut. J. R. Aeronaut. Soc. 74 (714) (1970) 517–532.
[7] Brown, W.F. and Srawley, J.E., Plane strain crack toughness testing of high strength metallic materials. West Conshohocken: ASTM, 1966.
[8] H. Tada, P.C. Paris, G.R. Irwin, The Stress of Crack Handbook, ASTM, 2000.
[9] J.C. Newman, Fracture analysis of surface- and through-cracked sheets and plates, Eng. Fract. Mech. 5 (1973) 667–689.
[10] J.C. Newman, I.S. Raju, An empirical stress-intensity factor equation for the surface crack, Eng. Fract. Mech. 15 (1-2) (1981) 185–192.
[11] X.P. Huang, W.C. Cui, D.X. Shi, Calculation of fatigue life of surface cracks at weld toe of submarine cone-cylinder, J. Ship Mech. 6 (4) (2002) 62–68.
[12] B. Fu, J.V. Haswell, P. Bettess, Weld magnification factors for semi-elliptical surface cracks in fillet welded T-butt joint models, Int. J. Fract. 63 (1993) 155–171.
[13] D. Bowness, M.M.K. Lee, Prediction of weld toe magnification factors for semi-elliptical cracks in T-butt joint, Int. J. Fatigue 22 (2000) 369–387.
[14] D. Bowness, M.M.K. Lee, Weld toe magnification factors for semi-elliptical cracks in T-butt joints-comparison with existing solutions, Int. J. Fatigue 22 (2000) 389–396.
[15] Y. Han, X.P. Huang, W.C. Cui, The simplified calculation method of stress intensity factors of surface cracks in T-butt joint, Ship Build. China 47 (1) (2006) 1–11.
[16] D.J. Hayes, A practical application of buekner's formulation for determining stress intensity factors for cracked bodies, Int. J. Fract. Mech. 8 (2) (1972) 157–165.
[17] T. Nykänen, G. Marquis, T. Björk, Fatigue analysis of non-load-carrying fillet welded cruciform joints, Eng. Fract. Mech. 74 (3) (2007) 399–415.
[18] M.L. Williams, Stress singularities resulting from various boundary conditions in angular corners of plates in extension, J. Appl. Mech. 19 (1952) 526–528.
[19] P. Lazzarin, R. Tovo, A unified approach to the evaluation of linear elastic stress fields in the neighborhood of cracks and notches, Int. J. Fract. 78 (1996) 3–19.
[20] P. Lazzarin, R. Tovo, A notch stress intensity factor approach to the stress analysis of welds, Fatigue Fract. Eng. Mater. Struct. 21 (1998) 1089–1103.

[21] P. Lazzarin, P. Livieri, Notch stress intensity factors and fatigue strength of aluminium and steel welded joints, Int. J. Fatigue 23 (2001) 225–232.

[22] W. Shen, N. Barltrop, R.J. Yan, E.Q. Liu, K. Qin, L.F. Song, Stress field and fatigue strength analysis of 135-degree sharp corners under tensile and bending loadings based on notch stress strength theory, Ocean Eng. 107 (2015) 32–44.

[23] W. Shen, R.J. Yan, N. Barltrop, P. Yang, E.Q. Liu, K. Qin, Stress field analysis of 135-degree sharp corners based on notch stress strength theory, J. Ship Mech. 19 (3) (2015) 273–283.

[24] L. Xu, B.Q. Lou, N. Barltrop, Considerations on the fatigue assessment methods of floating structure details, J. Eng. Marit. Environ. 227 (3) (2013) 284–294.

[25] W. Shen, Stress Field and Fatigue Strength Assessment of Ship Welded Joints Based On Singular Strength Theory, Wuhan University of Technology, Wuhan, 2015.

[26] Hobbacher. A., Recommendations on fatigue of welded components. IIW Document XV-845-96, 1996.

[27] Welding Standards Policy Committee. Fatigue design and assessment of steel structures. British Standard 7608, 1993.

[28] T.R. Gurney, The Influence of Thickness On the Fatigue Strength of Welded Joints, Abington Publishing, Cambridge, 1979.

[29] P. Dong, A structural stress definition and numerical implementation for fatigue analysis of welded joints, Int. J. Fatigue 23 (10) (2001) 865–876.

[30] T.R. Gurney, The Fatigue Strength of Transverse Fillet Welded Joints, Abington Publishing, Cambridge, 1991.

[31] K.M. Engesvik, T. Moan, Probabilistic analysis of the uncertainty in the fatigue capacity of welded joints, Eng. Fract. Mech. 18 (4) (1983) 743–762.